Use of an Accurate DNS Method to Derive, Validate and Supply Constitutive Equations for the MFIX Code

Zhi-Gang Feng

Students: Yifei Duan (presenter), Cenk Sarikaya, Miguel Ponton, Samuel Musong.

Univ. of Texas at San Antonio

Friday, April 22, 2016

Supported by: DOE-NETL (Grant #: DE-FE0011453)

Multiscale Modeling for Particlulate Flows

Resolved Discrete Particle
(Direct Numerical Simulation)
Model

Unresolved Discrete Particle
(Discrete Element)
Model

Two-Fluid
(Continuum)
Model

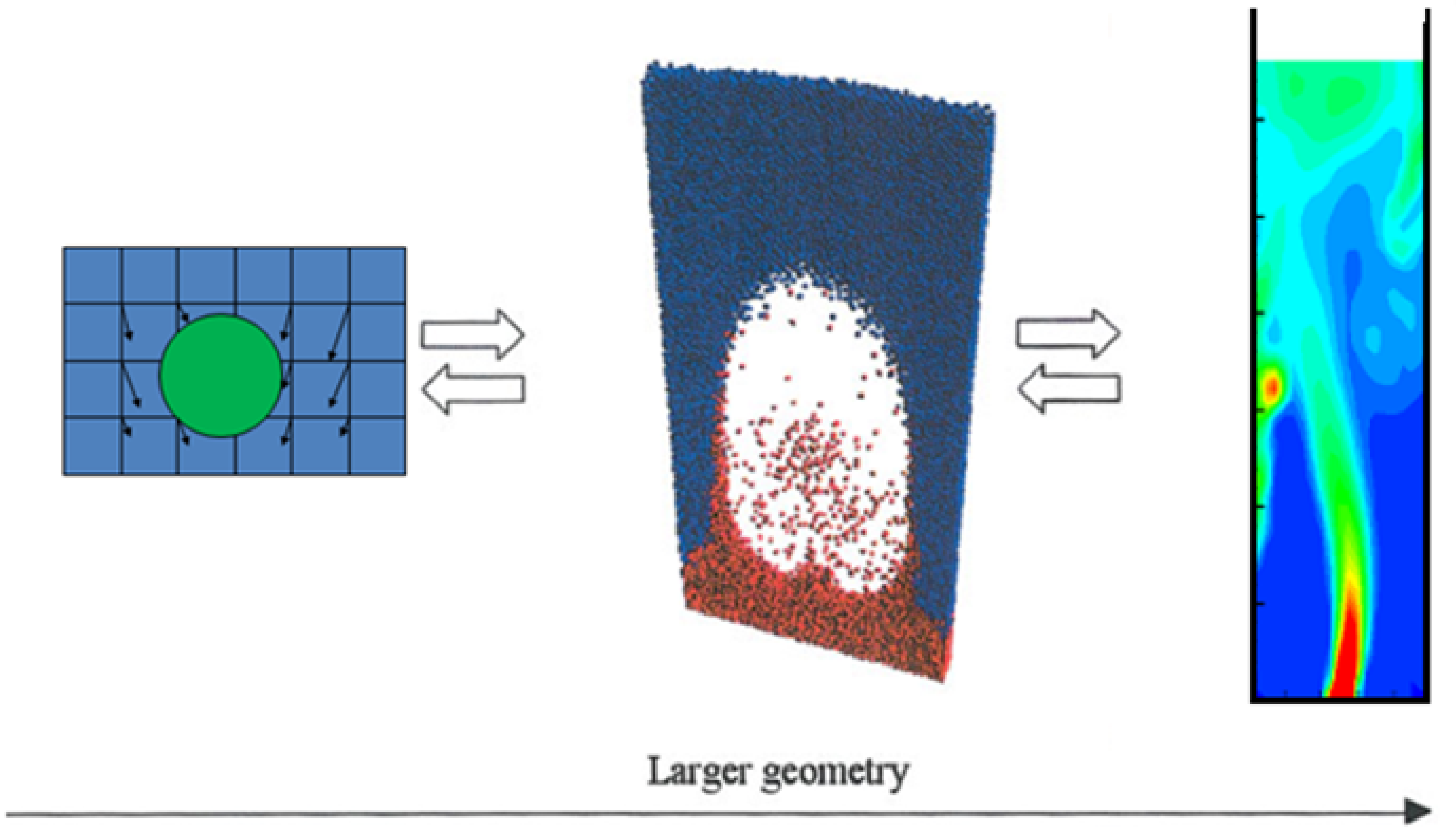

DNS simulation method: Proteus*

- Fluid velocity and pressure fields
  - Lattice-Boltzmann method; fixed regular grid.
- Particle-fluid interactions
  - Immersed boundary method; moving boundary nodes
- Particle-particle interactions
  - Soft-sphere collision scheme
  - Hybrid repulsive-force/lubrication scheme
- Particle dynamics
  - Newton's equations of motion (translational and rotational motions)

*Feng, Z.-G. and E. E. Michaelides, "***Proteus***: A direct forcing method in the simulations of particulate flow," *J. Comput. Phys.*, **202**: 20-51 (2005).

Interface momentum and heat transfer

- Interface models in MFIX
  - Most of them based on experimental studies at high solid fractions.

  DRAG:
  - Ergun model
  - Wen-Yu model
  - Gidaspow model
  - Syamlal and O'Brien model
  - Hill-Koch-Ladd model

  HEAT TRANSFER:
  - Gunn model
  - Sun model

Some existing correlations

- Carman-Kozeny equation
  - Based on experiments, for slow flows

$$\nabla p = -\frac{180\phi^2}{(1-\phi)^3 d^2}\mu U$$

  - Dimensionless drag

$$F(\phi,0) = 10\frac{\phi}{(1-\phi)^2}$$

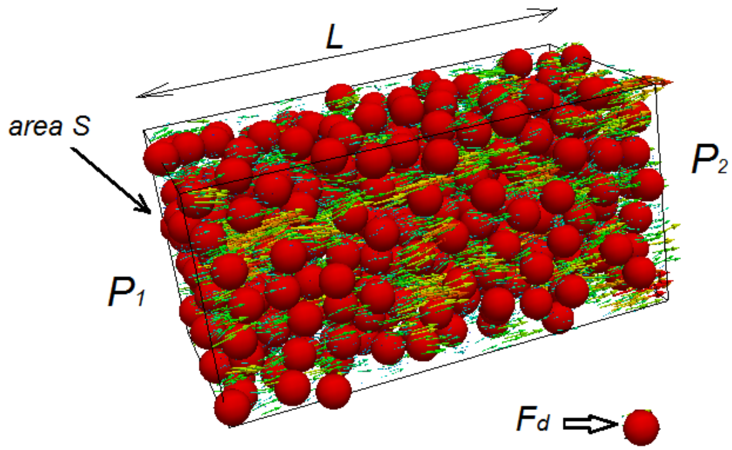

- Ergun equation, based on experiments

$$F(\phi,\mathrm{Re}) = 8.33\frac{\phi}{(1-\phi)^2} + \frac{0.097}{(1-\phi)^2}\mathrm{Re}$$

Validation case: Flows over face-centered arrays of spheres

- A small cubic unit of size L is selected as computational domain.
  - Low Reynolds number (Re<0.01)
  - solid volume fraction $\phi = \frac{16\pi a^3}{3L^3}$
    - Highest solid fraction is 0.74 when spheres are in contact.
    - We are able to achieve converged results at solid fraction 0.658.
  - Grid up to 200x200x200 is used
    - Particle diameter is outlined by 136 nodes;
    - 57837 nodes assigned to the surface of a sphere
  - Dimensionless drag force

$$F = \frac{F_d(\phi)}{F_d(0)} = \frac{F_d(\phi)}{6\pi\mu a U}$$

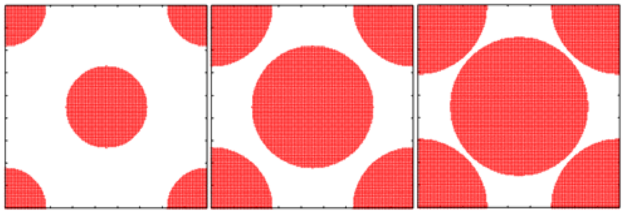

The void region(white) and solid region at a side surface of the computational cell Left: Φ=0.134; middle: φ=0.452; right: φ=0.659

- Theoretical solution for Stokes flows at low solid fraction(<0.2)*

$$F = \frac{1-\phi}{1 - 1.791\sqrt[3]{\phi} + \phi - 0.302\phi^2 + \cdots}$$

Hasimoto, H., "On the periodic fundamental solutions of the Stokes equations and their application to viscous flow past a cubic array of spheres," *J. Fluid Mech.*, 5:317-328 (1959).

Validation results

- Flow structures for face-centered cases

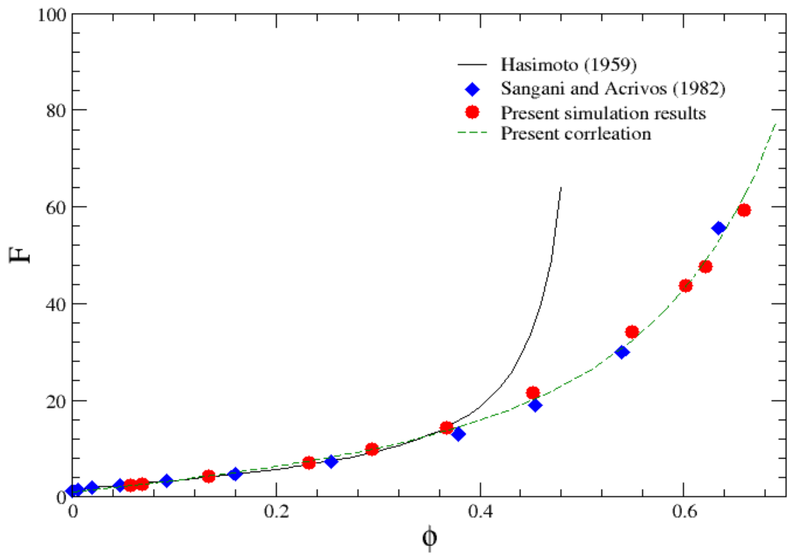

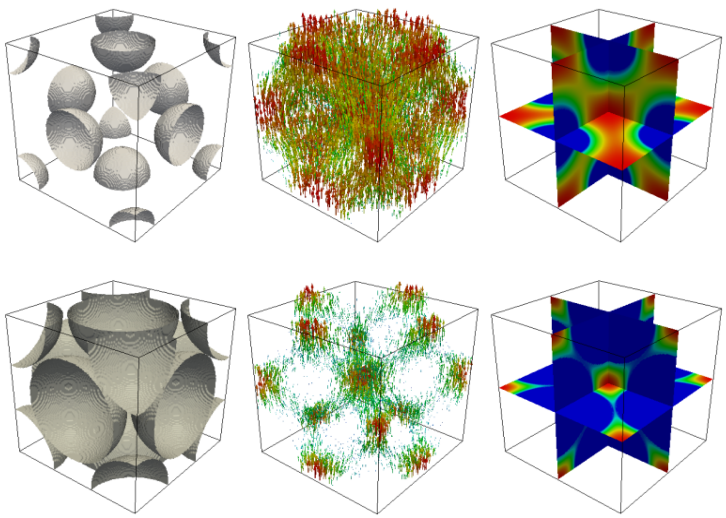

Flow over face-centered arrays of spheres at solid fractions 0.134 and 0.659: (a) pore structure; (b) flow velocity vector; (c) flow velocity (magnitude) contour.

- Correlation of $C_d \sim \varphi$

$$F(\phi) = 10\frac{\phi}{(1-\phi)^2} + 12\phi\sqrt{1-\phi} + 1.$$

Flows over random arrays of spheres

- Randomly distributed spheres
  - Using 60~405 spheres; solid fraction Φ=0.05~0.63.
  - Different Reynolds number by changing pressure gradients, 0<Re<300.

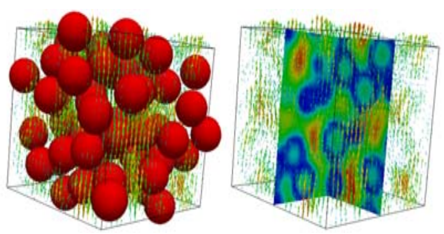

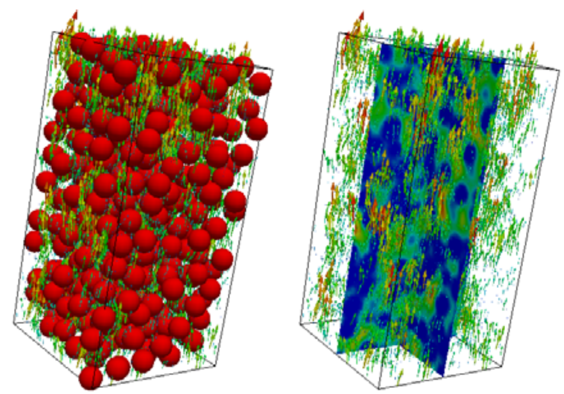

LEFT: Flow over a random distributed 60 spheres; RIGHT: Flow over 405 spheres. The same pressure gradients are applied. Solid volume fraction for both cases: φ=0.345.

Influence of sphere configurations

- Three different random configurations of 50 spheres placed in a cube (solid fraction 0.2873)
- Applied the same pressure gradient

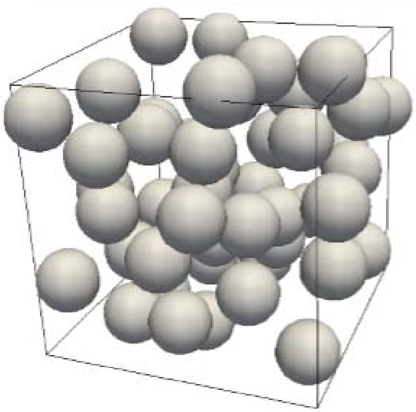

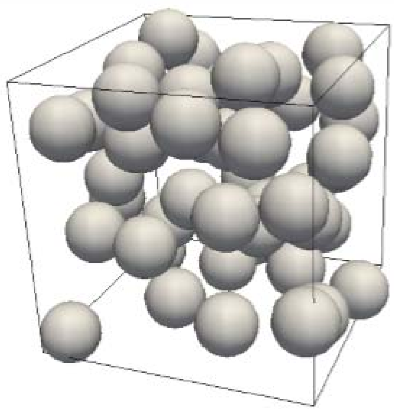

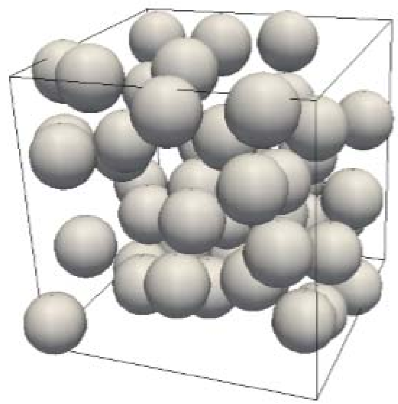

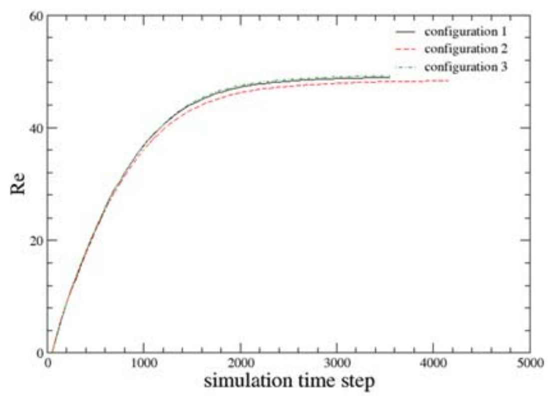

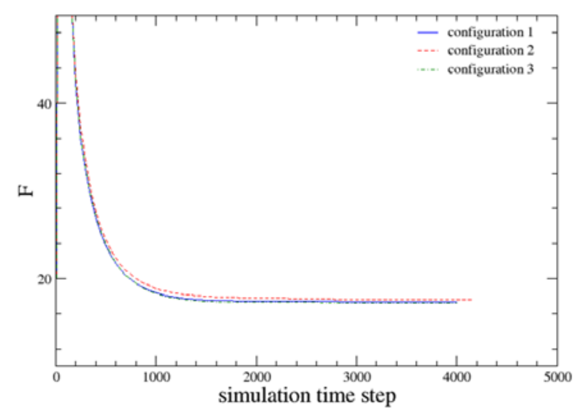

There exists a general drag model for random arrays of spheres

Drag vs. solid fraction and Reynolds number

- In general, it is found $F = F_0 + m\,\mathrm{Re}$
  - F_0 and m are only functions of solid fraction.

- At very low Re<<1, $F_0 = 1 + 9.5\phi/(1-\phi)^3 + 9.5\phi(1-\phi)^3$

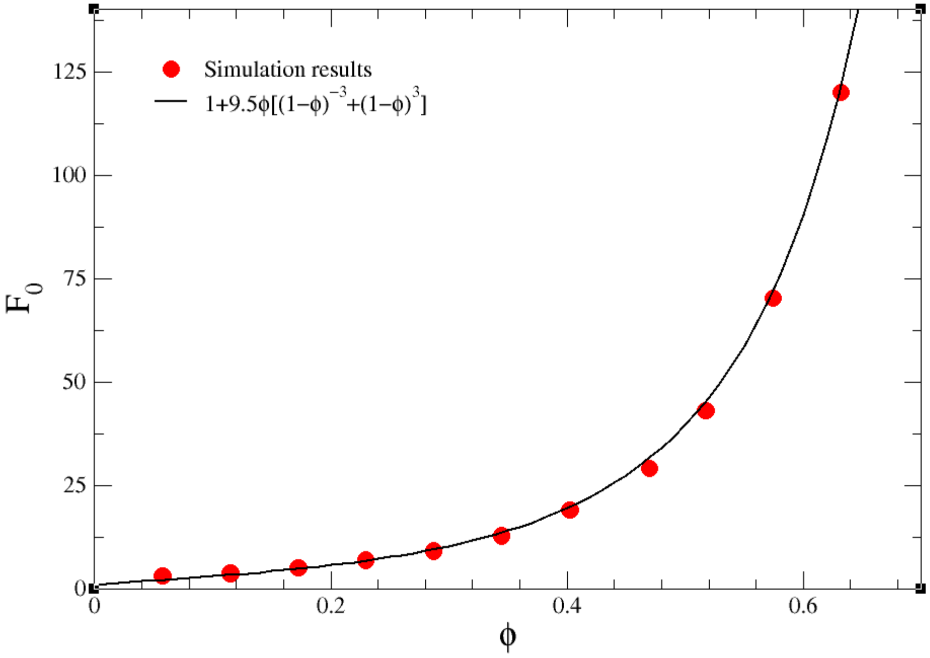

Drag vs solid fraction and Reynolds number

- Slope m for each solid fraction

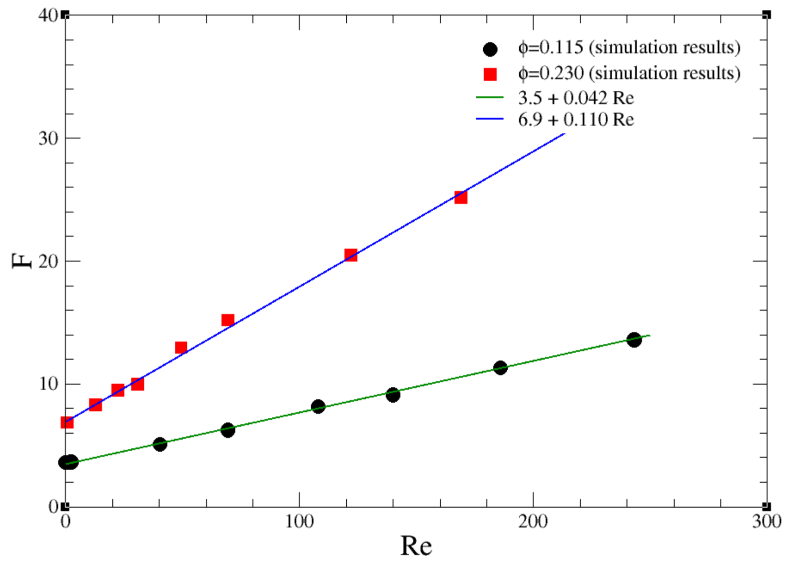

- Slope vs. solid fraction

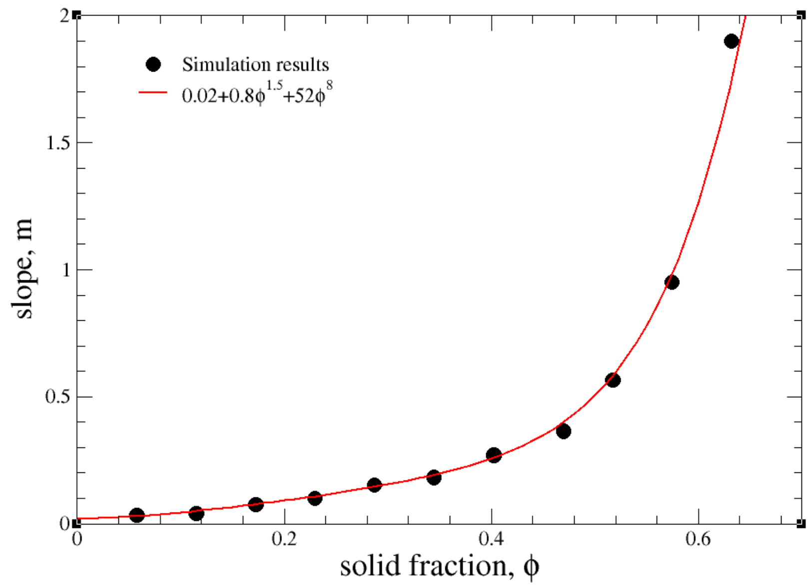

$$m = 0.002 + 0.8\phi^{1.5} + 52\phi^{8}$$

New drag correlation

- Final correlation for the drag model:

$$F = 1 + 9.5\varphi/(1-\varphi)^3 + 9.5\varphi(1-\varphi)^3 + (0.002 + 0.8\varphi^{1.5} + 52\varphi^8)\,\mathrm{Re}$$

  – Based on over 150 simulation data.

  – Applicable to solid fraction 0.05~0.63 and

  – Easy to be implemented in MFIX

Comparison with other models

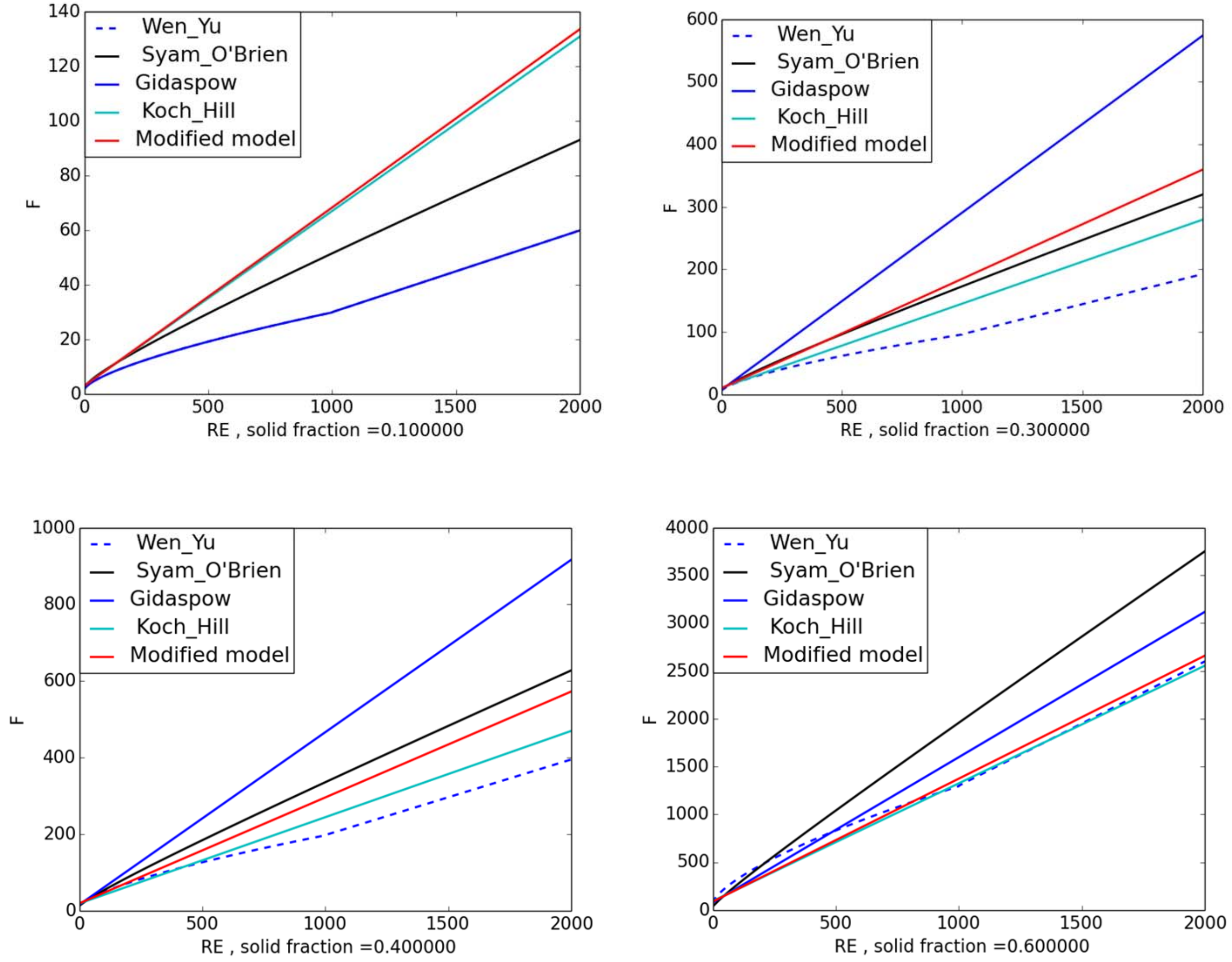

The nondimenstional drag force vs. Reynolds number at four different solid volume fractions

Implementation of drag model

SIMULATION AND MODEL PARAMETERS	
Bed height	90cm
Bed width	15cm
Static bed height	30cm
Grid resolution	30x90
Gas density	1.205x10-3g/cm3
Gas viscosity	1.8x10-5 Pa S
Particle density	270 0g/cm3
Particle diameter	0.4cm
Initial volume fraction	0.62
Angel of internal fraction	30
Restitution coefficient	0.9
Friction coefficient	0.3
Background velocity	2.6m/s

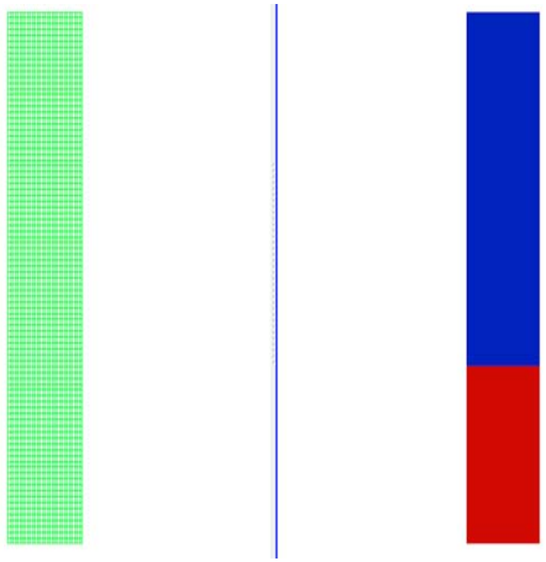

Tsuji, Y., et al. (1993). "Discrete particle simulation of two-dimensional fluidized bed." Powder technology **77**(1): 79-87.

Bubble dynamics in fluidized bed

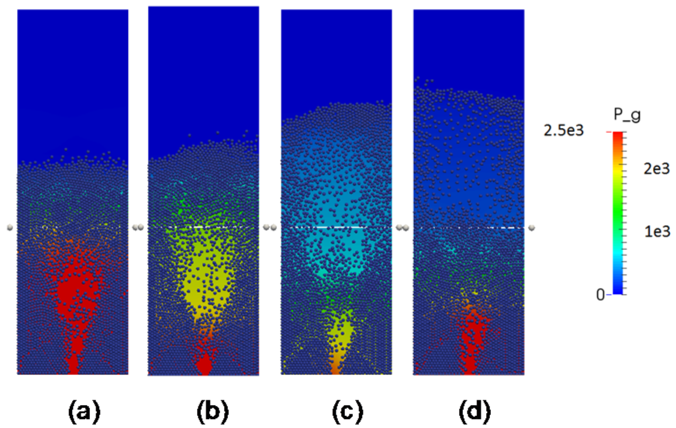

Formation of a bubble in a fluidized bed from DEM simulation. Gas pressure is shown in color, measured pressure changed from maximum value (a) to minimum value (d) in a cycle. (b), (c) and (d) are snapshots 0.04s, 0.14s, and 0.23s after snapshot (a).

Pressure fluctuation measured at 20 cm bed height

Pressure from peak to bottom in a cycle caused by bubble burst

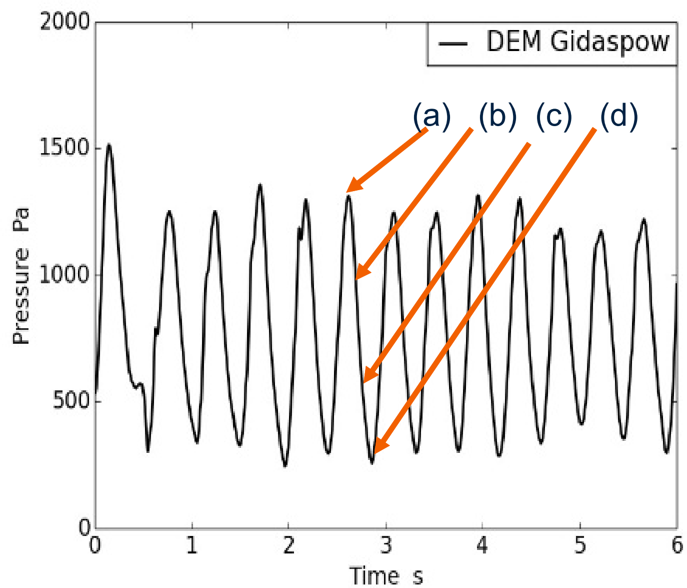

Pressure at 20cm bed height along with time

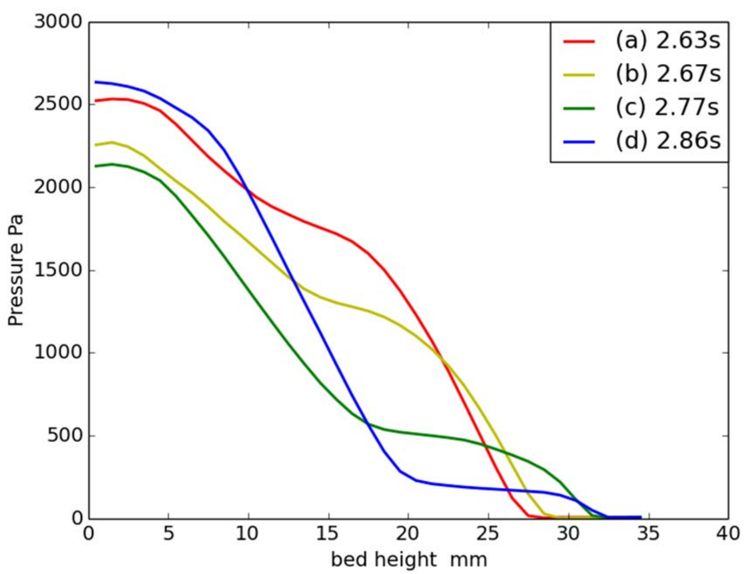

Gas pressure along with bed height, corresponding to the four snapshots at different time in Figure

Comparison with experimental data

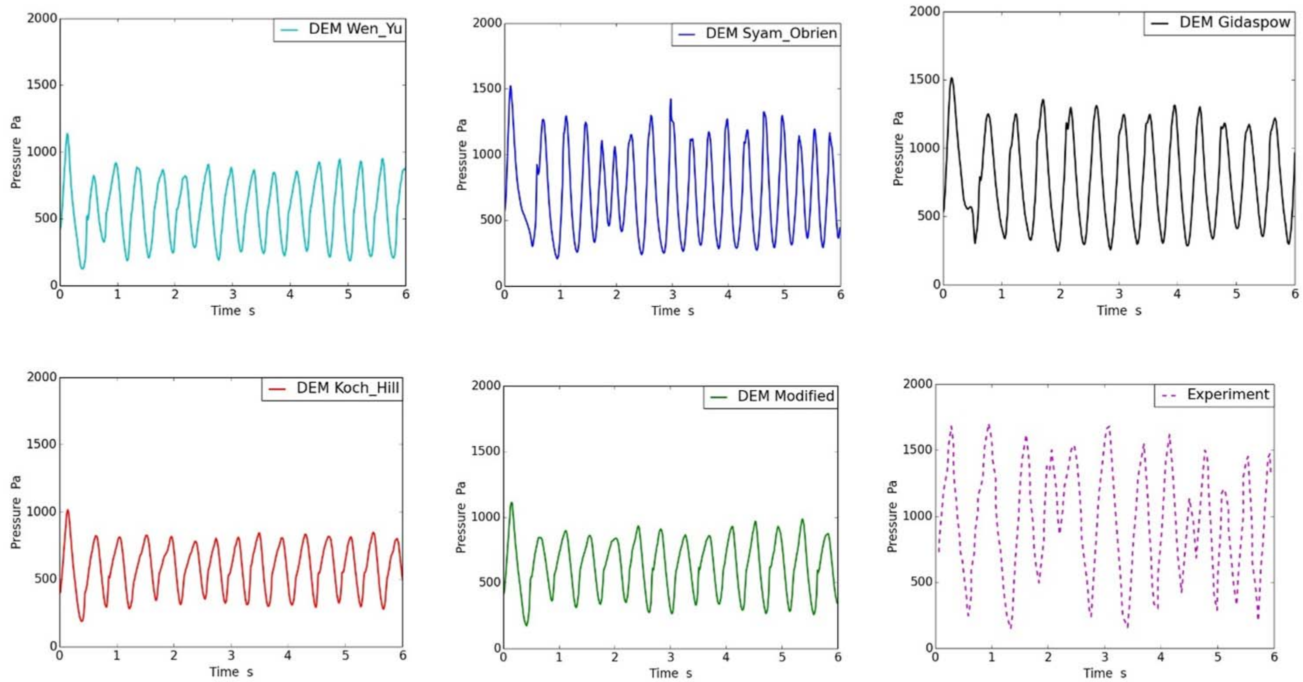

Gas pressure at 20 mm bed height from DEM simulation of five drag models and experimental data.

Data based on DEM simulation compared with experimental result

DRAG MODEL	Number of Bubbles observed in 6 secs	Avg Max pressure at 20mm (Pa)	Avg Max Difference	Avg Min pressure at 20mm (Pa)	Avg Min Difference	Avg pressure	Avg Pressure Difference	Max Bed Height(mm)	Avg Bed Height(mm)
Wen-Yu	15	897.07	-41%	227.13	-40%	570.06	-40.26%	33	29
Syam-Obrien	18	1221.61	-19%	306.04	-20%	713.96	-25.18%	43	31
Gidaspow	13	1276.92	-16%	320.57	-16%	777.58	-18.52%	42	32
Koch-Hill	14	829.66	-45%	307.58	-19%	588.26	-38.36%	31	27
Modified	13	914.42	-39%	300.94	-21%	630.01	-33.98%	33	28
Experiment	12	1511.32	0%	380.92	0%	954.29	0%		

Result comparison between DEM and TFM

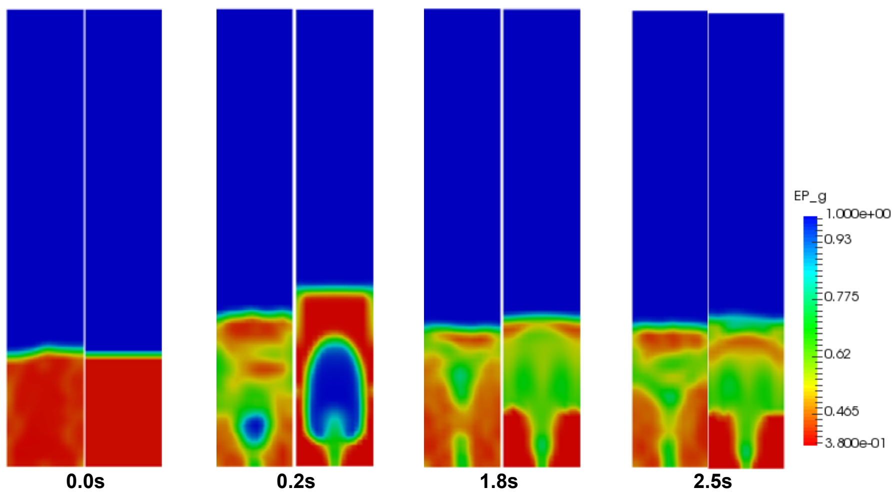

Simulation snapshots: Gas volume fraction at different time using Modified drag model. (Left: DEM results ; Right: TFM results)

TFM can predict the structure of flow field quite well. However in the region where solid volume fraction is very high (>0.6), the TFM still is not able to accurately capture the realistic particle interaction as seen in DEM simulations

Averaged measured pressure generally agrees with the results of DEM simulations

Fluctuation frequency is higher in TFM compared with DEM , also the amplitude is much smaller than that observed in DEM

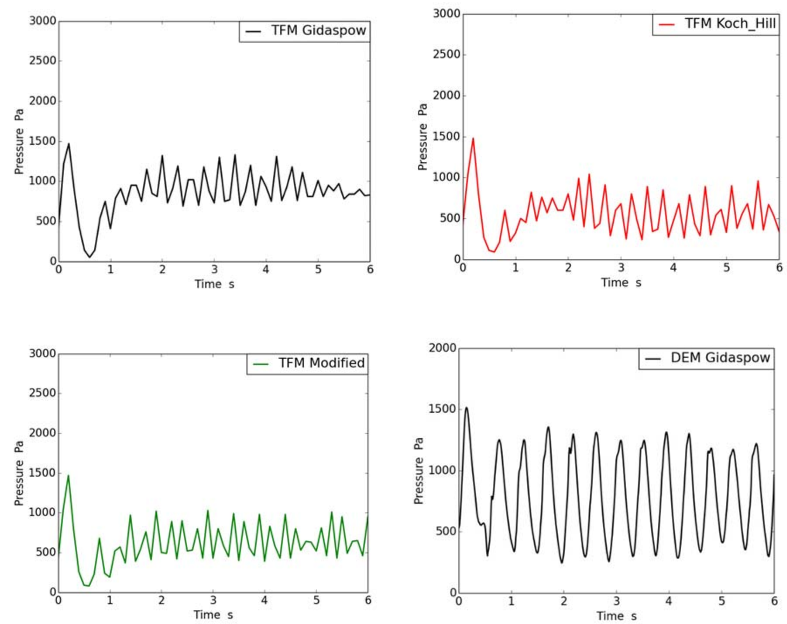

Gas pressure at 20 mm bed height from TFM simulation (solid line) and experimental data (dashed line)

Interphase heat transfer model

Current heat transfer model: Gunn's model

Interphase heat transfer

$$\gamma_{gm} = \frac{C_{pg} R_{gm}}{\left[\exp\left(\frac{C_{pg} R_{gm}}{\gamma_{gm}^0}\right) - 1\right]}$$

$$\gamma_{gm}^0 = \frac{6\kappa_g \varepsilon_m Nu_m}{d_m^2}$$

$$Nu_m = \left(7 - 10\varepsilon_g + 5\varepsilon_g^2\right)\left(1 + 0.7\,\mathrm{Re}_m^{0.2}\,\mathrm{Pr}^{1/3}\right) + \left(1.33 - 2.4\varepsilon_g + 1.2\varepsilon_g^2\right)\mathrm{Re}_m^{0.7}\,\mathrm{Pr}^{1/3}$$

Modified Nussle number derived from PR-DNS given by Sun*
Correlation valid in the bed porosity range 0.5~1.0, and 1<=Re<=100.

$$\mathrm{Nu} = (-0.46 + 1.77\varepsilon_b + 0.69\varepsilon_b^2)/\varepsilon_b^3 + (1.37 - 2.4\varepsilon_b + 1.2\varepsilon_b^2)\mathrm{Re}^{0.7}\mathrm{Pr}^{1/3}.$$

Summary of MFIX Equations (January 2012), NETL.

*Sun, B., et al. (2015). "Modeling average gas–solid heat transfer using particle-resolved direct numerical simulation." International journal of heat and mass transfer 86(0): 898-913.

Predicted gas temperature using different combination of closure laws

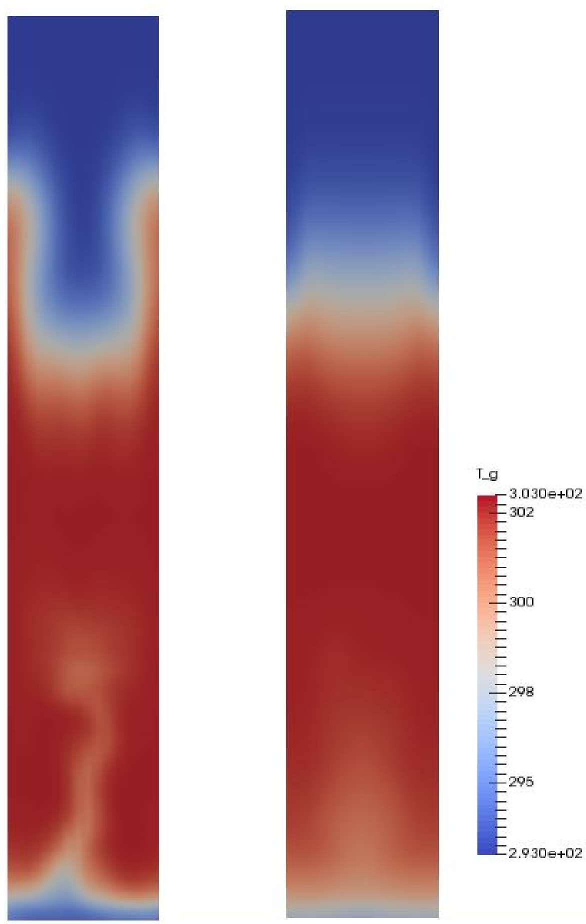

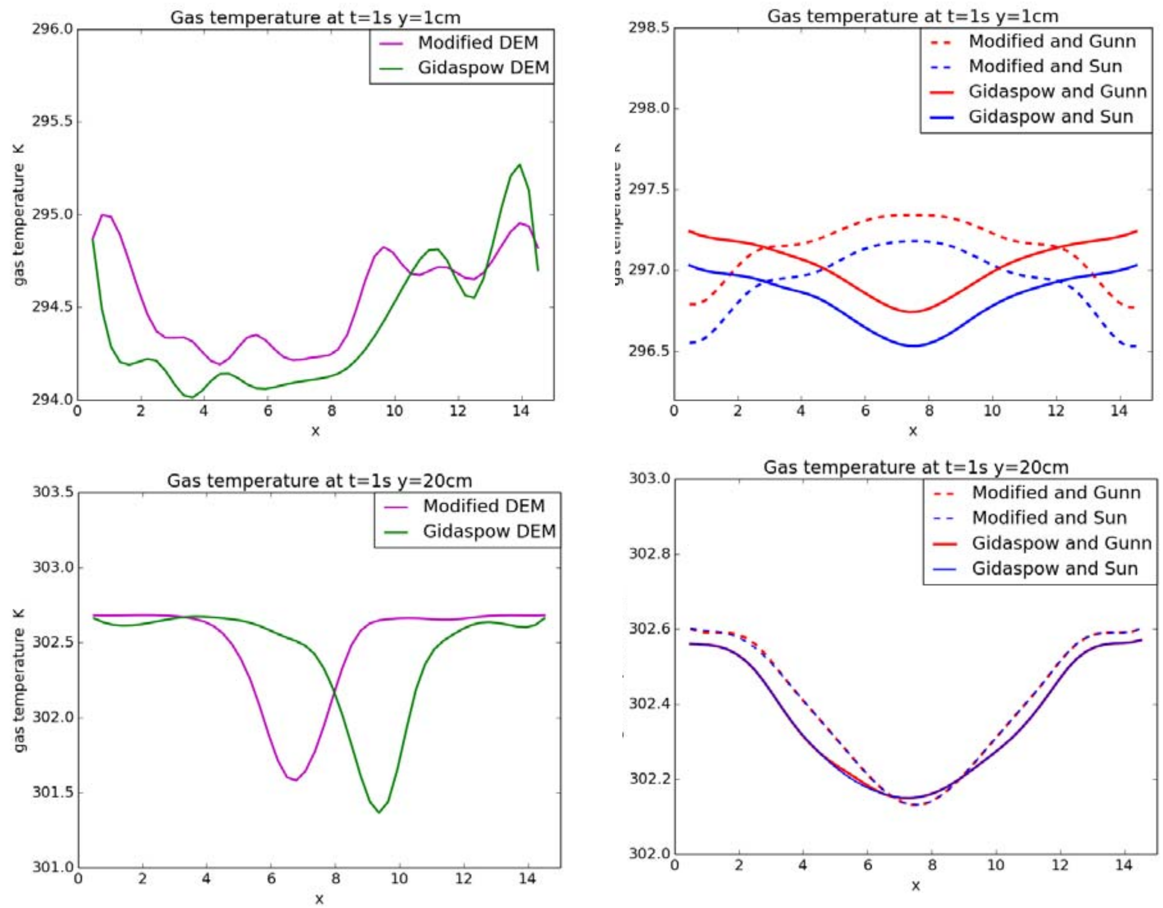

Gas temperature field from DEM (left) and TFM (right)

Temperature at 1cm bed height and 20cm bed height using different combination of closure laws

Drag model affect temperature field by affecting the flow structure

Different heat transfer models have larger impact on area near the bottom inlet

Summary and future work

Gas–solid flow behavior in a horizontal pipe after a 90^o vertical-to-horizontal elbow
A layer of high solid volume fraction flow near the top wall
Study the effect of different constitutive equations and boundary conditions

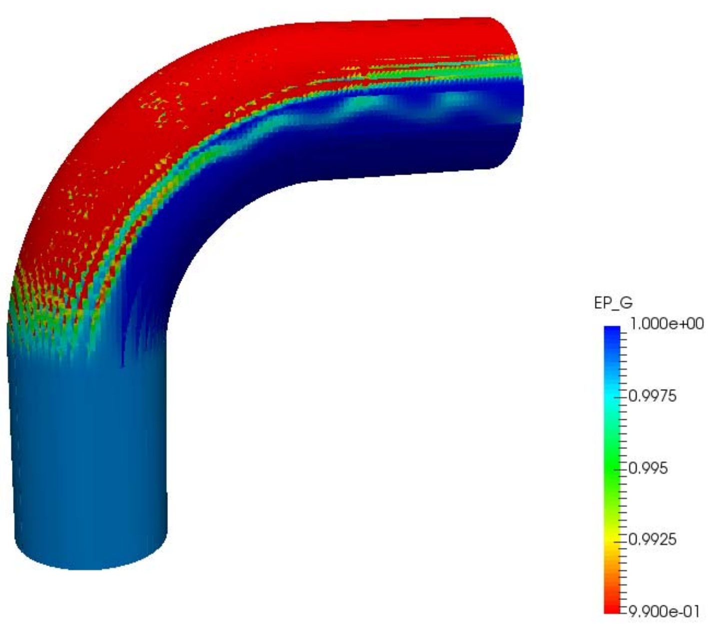

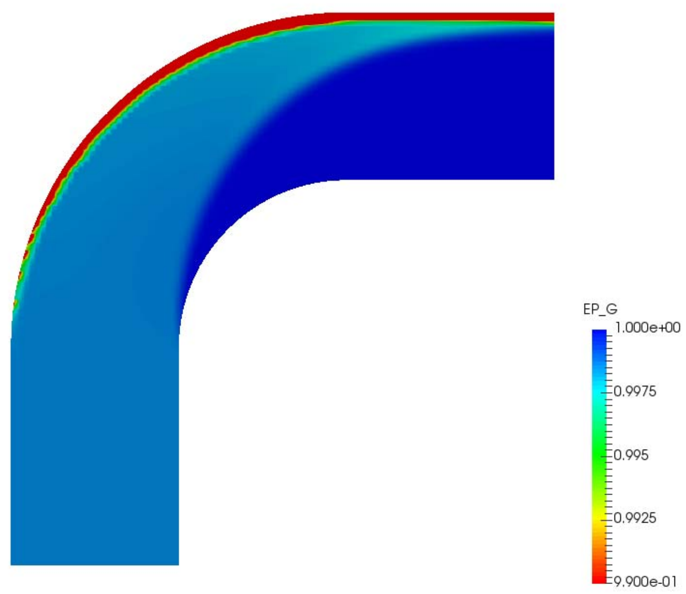

Summary and future work

- DNS based *Proteus* method is extended to solve heat transfer
- Follow the same procedures of deriving drag model to develop new closure law for interphase heat transfer (in progress)
- Work in progress

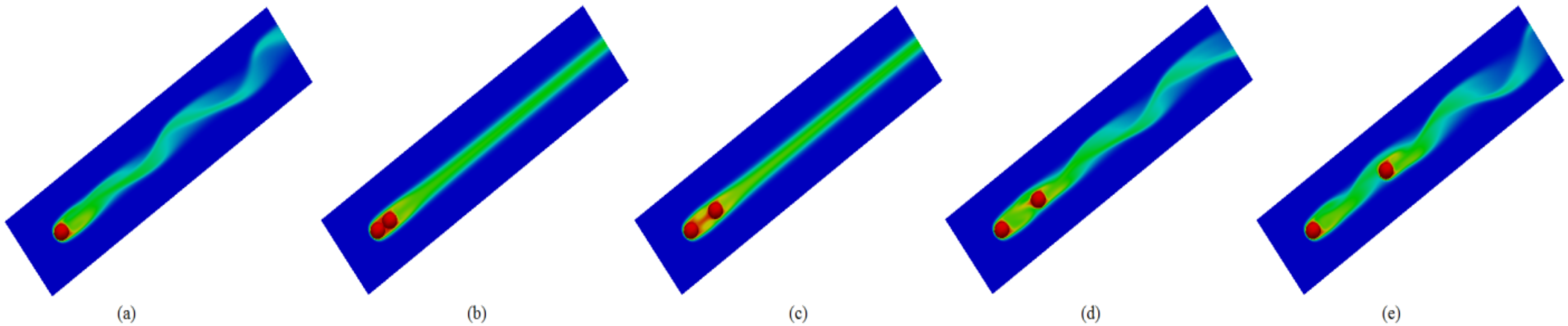

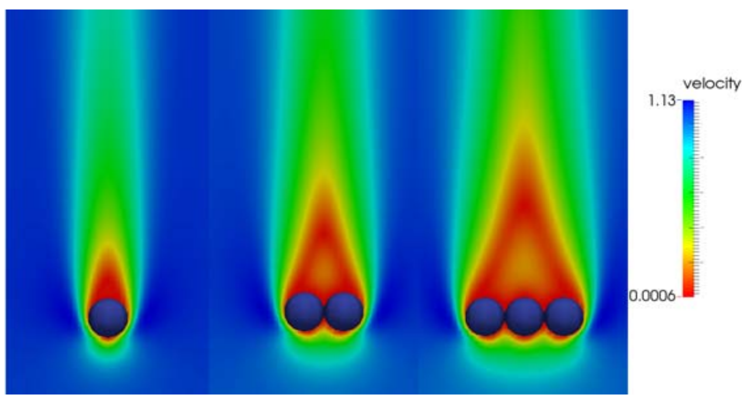

Summary and future work

- A new drag model has been developed and implemented in MFIX
- DEM simulation predicted result more close to experimental data
- Choice of drag/heat transfer model can significantly influence MFIX simulation results

Thank you